Osteoking improves OP rat by enhancing HSP90-β expression

YAN SUN[1-3*], RAN CHEN[4*], DI ZHU[1,2], ZHI-QIANG SHEN[1], HONG-BIN ZHAO[3] and WEN-HUI LEE[2*]

[1]Pharmaceutical College and Key Laboratory of Pharmacology for Natural Products of Yunnan Province, Kunming Medical University, Kunming, Yunnan 650500; [2]Key Laboratory of Bio-Active Peptides of Yunnan Province/Key Laboratory of Animal Models and Human Disease Mechanisms of The Chinese Academy of Sciences, Kunming Institute of Zoology; [3]The Emergency Department, The First People's Hospital of Yunnan Province/The Affiliated Hospital of Kunming University of Science and Technology, Kunming, Yunnan 650032; [4]The Clinical Laboratory Department, The Second Affiliated Hospital of Kunming Medical University, Kunming, Yunnan 650000, P.R. China

Received October 5, 2019; Accepted February 27, 2020

DOI: 10.3892/ijmm.2020.4529

Abstract. Osteoporosis (OP) is a chronic bone disease that affects individuals worldwide. Osteoporosis is primarily asymptomatic, and patients with OP suffer from pain, inconvenience, economic pressure and osteoporotic fracture (OPF). Osteoking, a Traditional Chinese Medicine compound that originates from the Yi ethnic group, has been used for a number of years to treat fractures. In our previous study, osteoking exhibited therapeutic effects on rats with OPF by promoting calcium deposition. Based on bioinformatics and network pharmacology analyses of a component-target-disease database, heat shock protein HSP 90-β (HSP90-β), also known as HSP90-β, was identified to be a key target of osteoking in OP. High HSP90-β expression levels were observed in osteoporotic rats and rat bone mesenchymal stem cells (rBMSCs) following osteoking treatment. After 12 weeks of administration *in vivo*, there was increased bone mineral density (BMD) ($P<0.05$), increased bone alkaline phosphatase ($P<0.05$), and improved bone microstructure in the osteoking group compared with those of the negative control group. *In vitro*, increased calcium deposition in rBMSCs was observed after 4 weeks of osteoking treatment. These results suggest that the mechanisms of osteoking are closely associated with HSP90-β and activate the bone morphogenetic protein (BMP) signalling pathway, primarily through BMP-2. Osteoking treatment improves OP in rats by enhancing HSP90-β expression.

Correspondence to: Professor Zhi-Qiang Shen, Pharmaceutical College and Key Laboratory of Pharmacology for Natural Products of Yunnan Province, Kunming Medical University, 1168 Chunrong Street, Kunming, Yunnan 650500, P.R. China
E-mail: szq21cn@hotmail.com

Dr Hong-Bin Zhao, The Emergency Department, The First People's Hospital of Yunnan Province/The Affiliated Hospital of Kunming University of Science and Technology, 157 Jinbi Street, Kunming, Yunnan 650032, P.R. China
E-mail: 596829191@qq.com

*Contributed equally

Abbreviations: BMD, bone mineral density; BMC, bone mineral content; BALP, bone alkaline phosphatase; BPs, bisphosphonates; ERT, estrogen replacement; OVX, ovariectomized; PINP, procollagen I N-terminal peptide; rBMSC, rat bone mesenchymal stem cell; SERM, selective estrogen receptor modulator; TCM, Traditional Chinese Medicine

Key words: network pharmacology, osteoking, osteoporosis, heat shock protein 90-β, bone morphogenetic protein-2

Introduction

Osteoporosis (OP) is a chronic bone metabolism disease that is clinically characterized by both bone mass reduction and bone architecture alteration. OP increases bone fragility and fracture risk worldwide (1,2). With the ageing of the population, particularly in Asia, the number of individuals who are aged ≥65 is projected to be 9.3% in 2025 (3). Patients with OP and osteoporotic fracture (OPF) experience pain, inconvenience, low quality of life, high economic burdens and mortality (4-6).

For OP prevention, controlling the risk factors is necessary. Exercising, body mass index (BMI) monitoring, and taking vitamin D and calcium are effective methods. In addition, decreasing hyperkyphosis, and avoiding smoking, alcohol and OP-inducing medications are preventive measures for OP (7,8). The primary purpose of osteoporotic therapy is to decrease the risk of fracture. The relevant medications are classified into two groups, antiresorptive agents and anabolic agents, and include bisphosphonates (BPs), estrogen replacement therapy (ERT) agents, selective estrogen receptor modulators, and calcitonin (CT) (9). However, the drugs available at present have a number of adverse effects. ERT, for example, is associated with coronary heart disease, breast cancer, stroke and dementia (10,11), and CT leads to nausea and local inflammation (12).

Osteoking is a Traditional Chinese Medicine (TCM) compound originating from the Yi ethnic group in Yunnan that has been used to treat bone diseases for decades (13). Initially, osteoking was approved by the Chinese State Food and Drug

Administration in 2002 to treat femoral head necrosis, lumbar disc herniation and osteoarthritis in the clinic (14). In our previous study, osteoking improved these bone diseases by upregulating the gene expression of Runt-related transcription factor 2 and vascular endothelial growth factor (VEGF) in osteoporotic rabbit models (15-18). In clinical settings, osteoking prevents fracture in humans (19). Osteoking improves osteoporotic fracture in rats (20). Prevention of OP/OPF may be a new application for osteoking. However, its exact mechanisms *in vivo* and *in vitro* remains unclear.

With the development of bioinformatics and network-pharmacology analyses, in particular component characterization of TCM compounds, researchers can easily obtain data, including chemical components, biological targets, and even metabolic processes *in vivo*, including absorption, distribution, metabolism and excretion. Researchers can analyze the relevant gene data from the Gene Expression Omnibus (GEO) database to obtain disease-associated targets (21). Investigating the components of osteoking and its OP-associated targets by network pharmacology may help elucidate the mechanisms of action of osteoking (22). The present study aimed to reveal the mechanism of osteoking and provide a new strategy for OP or OPF therapy.

Materials and methods

Drugs and reagents. Osteoking was prepared according to the Chinese Pharmacopeia (China Pharmacopeia Committee, 2002) and was supplied by Crystal Pharma Co., Ltd. (lot. no. 20160506) (23). Its formula was as follows: *Citrus reticulata Blanco*, *Carthamus tinctorius* L., *Panax notoginseng* (Burk) F. H. Chen Ex C., *Eucommia ulmoides Oliv*., *Panax ginseng* C. A. Mey., *Astragalus membranaceus* (Fisch.) Bunge, and *Trionycis Carapace* (Fig. S1). The above materials were ground into a coarse powder, immersed in 10-fold distilled water for 12 h at room temperature and then boiled using a distillation apparatus for 1 h. This process was repeated twice, and for the second and third extraction, the residue from the previous extraction was filtered, and the same extraction procedures were applied. Thereafter, the combined extracts were filtrated and evaporated using a rotary evaporator at 50˚C to a relative density of 1.03 g/cm^3 and centrifuged (1,450 x g; 30 min; room temperature) and the obtained supernatant was centrifuged (1,450 x g; 30 min; room temperature) once again following precipitation for 12 h. Subsequently, 0.36 g/ml was the clinical concentration of crude osteoking used.

Recombinant human parathyroid hormone 1-34 (rhPTH 1-34) was obtained from Dailan Meilun Biotech Co., Ltd. (cat. no. MB1241), Chemical Abstracts Service (CAS ID: 52232-67-4).

The antibodies used were anti-β-actin clone AC-15 (1:5,000; cat. no. A1978; Sigma-Aldrich; Merck KGaA), anti-BMP-2 (1:2,000; cat. no. 18933-1-AP; ProteinTech Group, Inc.), anti-heat shock protein HSP 90-β (HSP90-β; 1:3,000; cat. no. 11405-1-AP; ProteinTech Group, Inc.), HRP-conjugated Affinipure Goat Anti-Mouse IgG (H+L; 1:5,000; cat. no. SA00001-1; ProteinTech Group, Inc.), HRP-conjugated Affinipure Goat Anti-Rabbit IgG (H+L; 1:5,000; cat. no. SA00001-2; ProteinTech Group, Inc.), and HRP-linked anti-Rabbit IgG (1:5,000; cat. no. G1215; 1:5,000; Wuhan Servicebio Technology Co., Ltd.).

OP model. All animal experiments were approved by the Animal Study Committee of Kunming Medical University (approval no. KMMU 2015007) and were conducted according to the requirements of the National Institutes of Health Guidelines for care and use of laboratory animals (24). A total of 62 female 3-month-old Sprague-Dawley rats (270±15 g; Dossy Co.) were maintained in standard conditions with a controlled temperature (21-23˚C) and a strict 12:12 h light: Dark cycle. All rats were fed standard rat chow and allowed *ad libitum* access to distilled water at all times during acclimation and experimental treatment periods. The health and behavior of rats was monitored every day. After 7 days of adaptation, animals were randomly divided into the bilateral ovariectomy (OVX) group (54 rats) and the sham-surgery group (8 rats). A total of 8 rats underwent bilateral adipose tissue resection, in which adipose tissue of a similar weight to the ovaries was removed (sham group), and the remaining 54 rats were subjected to bilateral ovariectomy (OVX rats). The animals were anesthetized with intraperitoneal injection of 30 mg/kg sodium pentobarbital (Servio Co.). Preoperatively, all animals were fasted for 12 h. Benzylpenicillin sodium (60,000 IU/kg; Harbin Pharmaceutical Co.) was administered for 3 consecutive days following the surgeries.

Experimental protocol. A total of 54 OP rats underwent OVX surgery, randomly selected from the OP animals (450±20 g), were randomly divided into three groups: A positive control group treated with 0.33 μg/kg/2 days *subcutaneous* (*s.c.*) rhPTH; a negative control group treated with 0.59 ml/kg *intragastric* (*i.g.*) 0.9% NaCl (Baxter Medicine Co., Ltd.); and osteoking group treated with 0.59 ml/kg i.g. osteoking. The dosage used for each animal was dependent on the weight and body surface area of the rat, as well as the conversion coefficient of the human clinical dosage for rats (25). After 12 weeks of treatment, the rats were sacrificed via cervical dislocation under deep anesthesia (intraperitoneal injection of 30 mg/kg sodium pentobarbital), as described previously. When animals were sacrificed, serum and bone were collected and preserved at -20˚C.

BMD analysis. After 4, 8 and 12 weeks of treatment with osteoking, the whole-body BMD was measured by dual-energy X-ray absorptiometry using the Lunar Prodigy Advance (GE Healthcare). Specific software for small animals (GE Medical Systems, enCORE2004 software; v.8.80.001) was used (26), as described previously.

Identification of active ingredients and prediction of OP-associated targets by bioinformatics. The Traditional Chinese Medicine Systems Pharmacology (TCMSP) Database (http://lsp.nwu.edu.cn/tcmsp.php) was used to obtain the main active ingredients of osteoking, which were identified using the cut-off values of oral bioavailability ≥30% and drug-likeness ≥0.18. The target-prediction model of TCMSP was used to predict the associated targets. Significantly different genes were obtained through the secondary mining of the GEO database (Gene accession numbers: GSE35955; GSE35958 and GSE35959) (27).

Cell culture. Rat bone mesenchymal stem cells (rBMSCs) were obtained from the Chinese Academy of Science Kunming Cell Bank of Type Culture Collection (Kunming Institute of Zoology, Chinese Academy of Sciences). The cells were maintained in Dulbecco's modified Eagle's medium (DMEM; Biological Industries) supplemented with 10% FBS (Biological Industries). The cells ($1x10^4$ in 200 ml/well) in 96-well plates and cultured in different concentration of osteoking. After 24 h of administration, the proliferations in each well were cultured with MTS colorimetric assay kit (Abcam Co., Ltd.) at 37˚C for 1 h and measured using a microplate reader (Tecan Group, Ltd.) on OD=490 nm (Fig. S2). Osteoking was filtered through a 0.22 mm filter and diluted 16 times for culture. The final concentration of osteoking was 22 g/l crude osteoking. There were two groups: The control group (DMEM+10% FBS) and osteoking group (22 g/l crude osteoking) for reverse transcription-quantitative polymerase chain reaction (RT-qPCR) and western blot analysis. The cells in 25 cm^2 culture flask were induced for 4 weeks. Concomitantly, the cells ($1x10^5$ in 1 ml/well) were divided into four groups: Control; 20 mmol/l HSP90-b inhibitor NVP-AUY922 (Selleck Chemicals); osteoking (22 g/l crude osteoking); and osteoking + HSP90-b inhibitor, and cultured in 6-well plates for 4 weeks. After 4 weeks of administration, the plates were stained by alizarin red at room temperature for 25 min and measured using a microplate reader.

Histopathology and immunohistochemistry. After 12 weeks of treatment, the 3rd lumbar vertebrae were harvested and fixed in 10% paraformaldehyde at room temperature for 14 days, dehydrated (60, 75, 95 and 100% ethyl alcohol) and decalcified (300 ml 30% HCL; 700 ml 4% paraformaldehyde; 140 g NaCl and 20 ml glacial acetic acid) gradually. Then, 5-μm-thick sections were prepared using a Leica RM2245 microtome (Leica Microsystems, Inc.). The anti-HSP90-β antibody (ProteinTech Group, Inc) was diluted 1:1,000 in blocking solution. After samples were washed 3 times in PBS, they were incubated with HRP-linked anti-Rabbit IgG (1:5,000; cat. no. G1215; Wuhan Servicebio Technology Co., Ltd.) at room temperature for 1 h. The results were analyzed using ImageJ software (version 1.46R; National Institutes of Health). The cells in six-well plates were washed and fixed using 10% paraformaldehyde at room temperature for 15 min. Alizarin red S (100 ml/bottle; Wuhan Servicebio Technology Co., Ltd.) was used at room temperature for 25 min and staining intensities were measured by microplate reader at an absorbance wavelength of 560 nm (Tecan Group, Ltd.).

Micro computed tomography (micro-CT) analysis. Following removal of adherent soft tissues, the bilateral femurs were preserved in 4% paraformaldehyde at room temperature as described previously (28). Micro-CT analysis was performed according to recent guidelines[56] using a micro-CT imaging system (Bruker microCT N.V.) with a spatial resolution of 17.75 μm (X-ray source 70 KV/357 μA; exposure time 250 msec; magnification, x15; 1.0 mm aluminum filter applied). Volumetric reconstructions and analyses were performed using built-in software NRecon 1.6 and CTAn 1.8 (Bruker microCT N.V.). The parameters measured were: Percent bone volume; bone surface/volume ratio (BS/BV); trabecular number (Tb.N); trabecular separation; trabecular thickness (Tb.Th); and structure model index (29).

Proteome analysis. After 12 weeks of treatment with osteoking, the protein expression levels of the osteoking group and the control group were measured by label-free quantification (Genecreate). The basic principle was based on the extraction peak area of the peptide segment parent ion. Then, the peptide segments and proteins in the sample were identified, and the identified peptide fragments/proteins were quantitatively analyzed. The two groups were designated as the osteoking group and the control group. Following removal of redundant sequences, the data contained 36,728 protein sequences from the UniProt database (30). The proteins were quantitatively analyzed by Skyline software (version 3.5; SkylineGlobal Co.), and the differences were identified using the cut-off |fold change| ≥2.

RT-qPCR. Total RNA from cells and tissue samples was separately isolated using TRIzol® reagent (Thermo Fischer Scientific, Inc.) according to the manufacturer's protocol. The primer sequences refer to the National Center for Biotechnology Information database (31) and were assessed by Oligo Calc. (http://biotools.nubic.northwestern.edu/OligoCalc.html) (32). The primers were designed as following: β-actin, forward 5'-TCTGAACCCTAAGGCCAACC-3', and reverse 5'-TACGTACATGGCTGGGGTGT-3'; Bmp-2, forward 5'-GTGCCCCCTAGTGCTTCTTAG-3', and reverse 5'-CAC CATGGTCGACCTTTAGGA-3'; Hsp 90-β, forward 5'-GCC CTGGACAAGATTCGGTA-3', and reverse 5'-ATCTTCAGC TCTTTCCCGCTG-3'. The thermocycling conditions: Initial denaturation is 95˚C for 30 sec; 30 of cycles of denaturation at 94˚C for 15 sec, annealing at 60˚C for 30 sec and elongation at 72˚C for 20 sec; and a final extension is 72˚C for 1 min). For RT-qPCR, cDNA was prepared from 2 μg RNA using a Prime Script RT Reagent kit (Takara Biotechnology Co., Ltd.) and analyzed with SYBR Green Master Mix (Takara Bio, Inc.) in an LC480 real-time PCR system (Roche Diagnostics). The data were quantified using the relative quantitative $2^{-\Delta\Delta Cq}$ method and were normalized to β-actin expression data (33).

Western blot analysis. Protein lysate (1 ml) with 10% PMSF (Dalian Meilun Biology Technology Co., Ltd.) was added into 100 mg bone or $1x10^6$ cells on the ice for 30 min. The samples were tested using BCA protein assay kit and adjusted as a same concentration 1 μg/ul. The loading quality of β-actin was 5 μl, and the loading quality of targets is 20 μl. Precast gel (4-20%) and PVDF were used. BSA (10%) blocked the PVDF at room temperature for 1 h. Anti-β-actin (1:5,000; cat. no. A1978; Sigma-Aldrich; Merck KGaA), anti-HSP 90-β (1:3,000; cat. no. 11405-1-AP; ProteinTech Group, Inc.) and anti-BMP-2 (1:2,000; cat. no. 18933-1-AP; ProteinTech Group, Inc.) were incubated at 4˚C overnight, as described previously. Then, 1:5,000 HRP-anti-Mouse (H+L; 1:5,000; cat. no. SA00001-1; ProteinTech Group, Inc.) or HRP-anti-Rabbit IgG (H+L; 1:5,000; cat. no. SA00001-2; ProteinTech Group, Inc.) was incubated at room temperature for 2 h. One PVDF was added with 1ml super HRP-reagent (Dalian Meilun Biology Technology Co., Ltd.) and displayed using an automatic chemiluminiscence system (Tanon Science and Technology

Figure 1. Components of osteoking. A total of 7 natural plants constitute osteoking.

Co., Ltd.). The degree of gray density was analyzed using Image J software (version 1.46R, National Institute of Health.).

Bio-layer interferometry (BLI). Biomolecular interactions were measured by the BLI method *in vitro* (34). All experiments were performed in 37˚C PBS and AR2G biosensors were used in ForteBio Octet Red 96 (ForteBio Inc.). All samples were added into the black 96-well plate (Greiner Bio-One Co., Ltd.). Before protein immobilization, the baseline was established with PBS prewetted AR2G biosensor. Then, HSP90-β and MGP (Matrix gla protein) were fixed to the AR2G biosensors at 0.1 mg/ml. The binding time was 600s and the dissociating time was 1,200 sec. The curve was fitted globally with a 1:1 model (Octet Red system; version 7.0).

Statistical analysis. All the experimental data were assessed using SPSS v21.0 statistical software (SPSS, Inc.), and the values are expressed as the mean ± standard deviation. Data distribution was determined by measuring kurtosis and skewness. Statistical significance was determined by a Student's t-test or ANOVA with Tukey's post hoc test. $P<0.05$ was considered to indicate a statistically significant difference.

Results

HSP90-β is the key target of osteoking in OP. In our previous studies, osteoking was identified to have positive effects on OP/OPF rats (19,23). The components of osteoking and its possible targets were obtained from the TCMSP database (Fig. 1). Notably, based on these targets, functional enrichments suggested that osteoking was associated with drug metabolic processes, blood circulation, hemostasis, circulatory system processes and VEGF (Fig. 2). These targets are indirectly associated with osteogenesis, but the related functions, including growth, repair and angiogenesis, may benefit OP/OPF. Based on gene data from the GEO database, the association between OP and osteoking focused on HSP90-β (Fig. 3A). Importantly, HSP90-β was also confirmed to be highly expressed, as determined by proteomic results in OP rat models (Fig. 3B). Thus, HSP90-β may be a key effector molecule of osteoking and serve an important role in the pathophysiological process of OP, as indicated by network-pharmacology analysis of the components of osteoking and the *in vivo* proteomic results.

Osteoking leads to calcification. Postoperatively, the total BMD values of rats in the OVX and sham groups were assayed

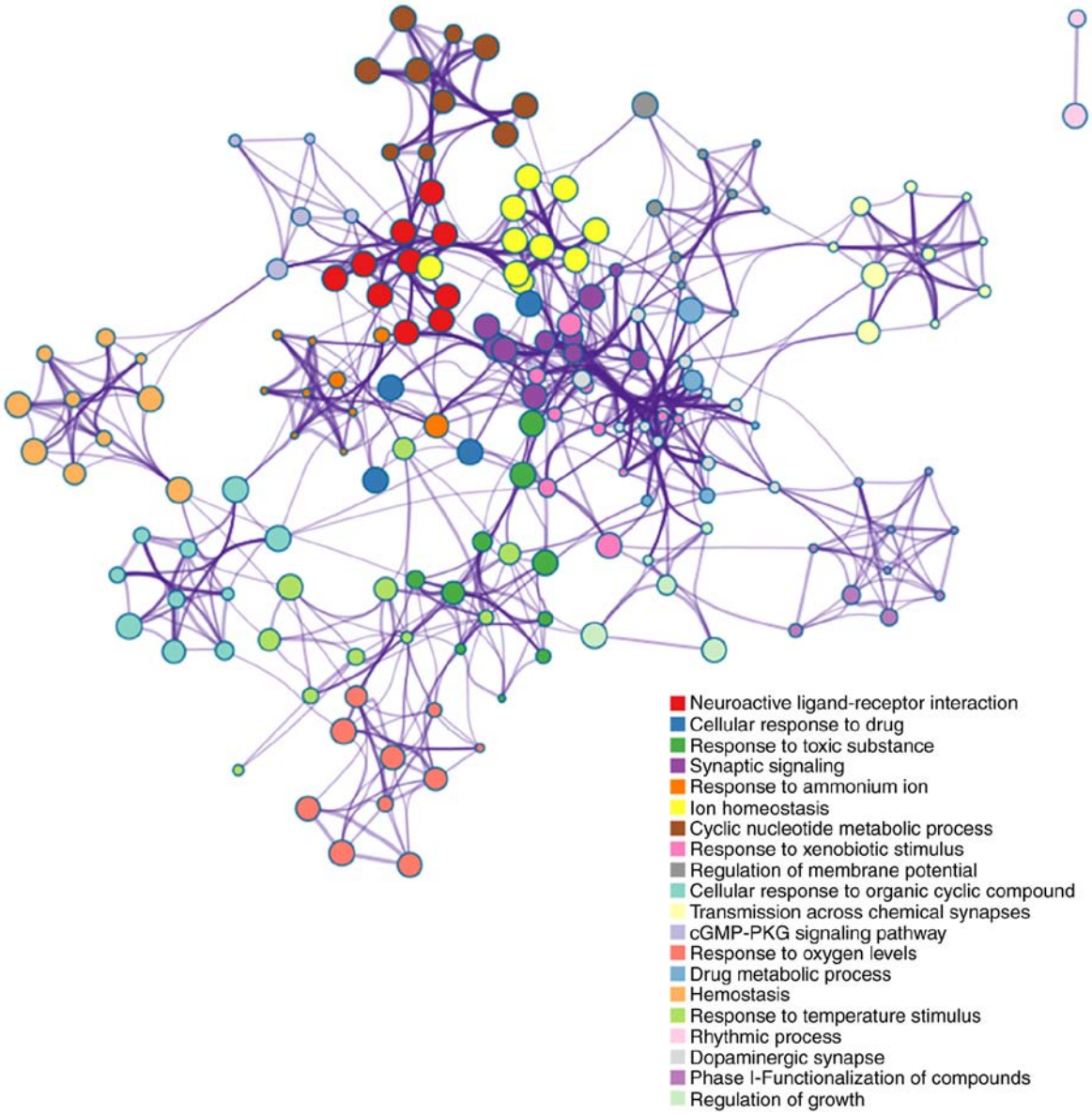

Figure 2. Functional enrichments of the relative targets of osteoking. The top 20 enriched signaling pathways from the Gene Ontology database.

using dual-energy X-ray. At the 23rd week, there was a significant difference (P<0.05) in BMD between the OVX group (0.177±0.006 g/cm^3) and the sham group (0.188±0.008 g/cm^3), suggesting that the OP rat model was successfully established. *In vivo*, the rat osteoporotic model was divided into three groups as aforementioned. Following treatment with osteoking, changes in BMD, which is the gold standard for evaluation of OP, were observed in each group (Fig. 4A). The BMD in the osteoking group significantly increased at the 8 and 12th weeks compared with that of the negative control group (P<0.05); however, the BMD in the osteoking group was decreased compared with that in the positive control group (P<0.05). After 12 weeks of administration, the micro-CT results indicated that the number of bone trabeculae increased in the osteoking group (Fig. 4B). The BS/BV ratio, Tb.Th and Tb.N in the osteoking group increased significantly compared with those of the negative control group (P<0.05; Fig. 4C). However, these parameters were all decreased compared with those in the positive control group (P<0.05). At the initial time, all osteoporotic rats in the three groups exhibited the same baseline bone alkaline phosphatase (BALP; 21.55±1.54 U/l), PINP (280.63±75.27 pg/ml) and tartrate-resistant acid phosphatase-5β (TRACP-5β; 0.71±0.01 mIU/ml) values. BALP and PINP were used as bone formation markers. The osteoking group demonstrated significantly increased BALP and PINP after 12 weeks of treatment with osteoking compared with those of the negative control group (P<0.05; Fig. 4D). In addition, in the osteoking group, TRACP-5β, a bone resorption marker, was decreased compared with in that of the other two groups.

HSP90-β improves OP by enhancing BMP-2 expression in vivo. After 12 weeks of treatment, osteoking led to calcification compared with that of the negative control group, and its mechanism was associated with HSP90-β (Fig. 5A). Osteoporotic rats in the osteoking group exhibited significantly increased HSP90-β expression levels (Fig. 5B). Moreover, increased BMP-2 expression levels were observed

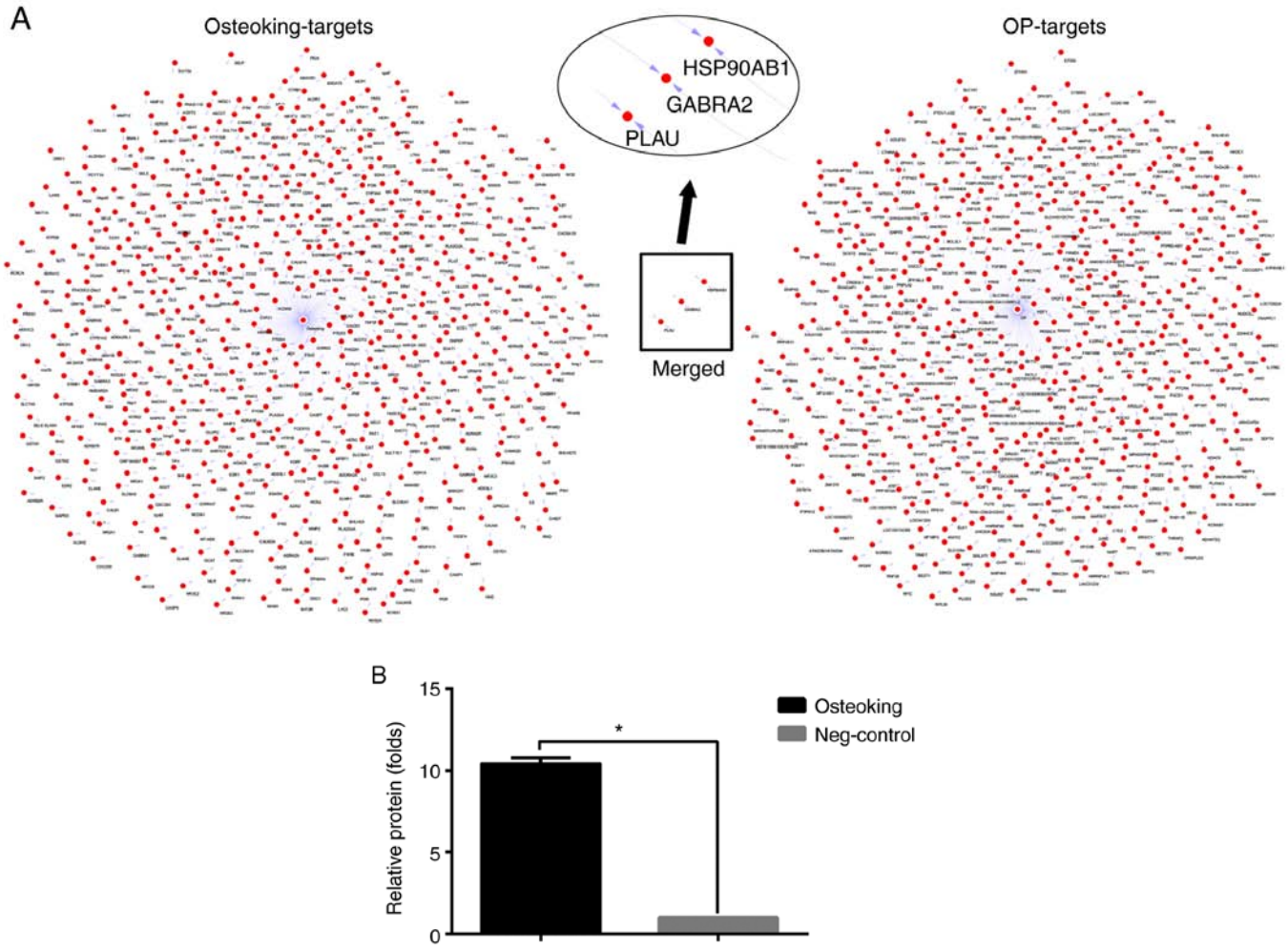

Figure 3. HSP90-β is a key target of the osteoking-mediated effects on osteoporosis. (A) The association between osteoporosis and osteoking, as determined by the Traditional Chinese Medicine Systems Pharmacology and Gene Expression Omnibus databases. (B) The difference in HSP90-β protein levels between the osteoking and negative control groups after 12 weeks of treatment with osteoking. The y-axis represents the fold change. The values are expressed as the mean ± standard deviation (n=6). *P<0.05. Neg-control, negative control.

in the osteoking group compared with those of the negative control group.

Osteoking leads to high expression of HSP90-β and BMP-2 after 4 weeks of culture in vitro. After 4 weeks of culture with osteoking, rBMSCs demonstrated similar *in vitro* results (Fig. 5C). HSP90-β expression was significantly increased in the osteoking group compared with that of the control group, and BMP-2 expression was also increased.

Blocking HSP90-β decreases calcium deposition. After 4 weeks of culture, inhibiting HSP90-β *in vitro* decreased calcium deposition in the osteoking + inhibitor group compared with the osteoking group (P<0.05; Fig. 6). The number of calcified nodules increased in the osteoking group compared with those of the control group (P<0.05). In addition, the osteoking + inhibitor group exhibited more calcified nodules compared with those of the control group (P<0.05).

Discussion

At present, bioinformatics has contributed to the development of TCM. Proteomics has validated the predicted results of network pharmacology. Moreover, this method accurately demonstrated marked changes between the osteoking and control groups.

In the present study, osteoking improved OP in rats, through increasing the BMD and enhancing the bone intensity. The micro-CT results demonstrated improved micro-structure in the osteoking group, which suggests an improved resistance to biomechanical force in OP rats, which would help to avoid fracture. Measurement of resistance to biomechanical force should have been used in this study instead of the micro-CT. Previous studies have indicated similar improvements of the OP/OPF model (13,15,18,19,20,23) and this is a limitation of the present study. Measurement of biomechanical force could be better to explain the effects of osteoking.

The results of the present study suggest that the key protein involved in osteoking-mediated effects on and the physiological process of OP is HSP90-β both *in vivo* and *in vitro*. After 12 weeks of administration, osteoporotic rats in the osteoking group had increased expression of HSP90-β compared with that of the negative control rats. The results demonstrated increased calcification and transiently increased osteogenic activity in the osteoking group compared with that of the negative control group. RBMSCs expressed increased HSP90-β

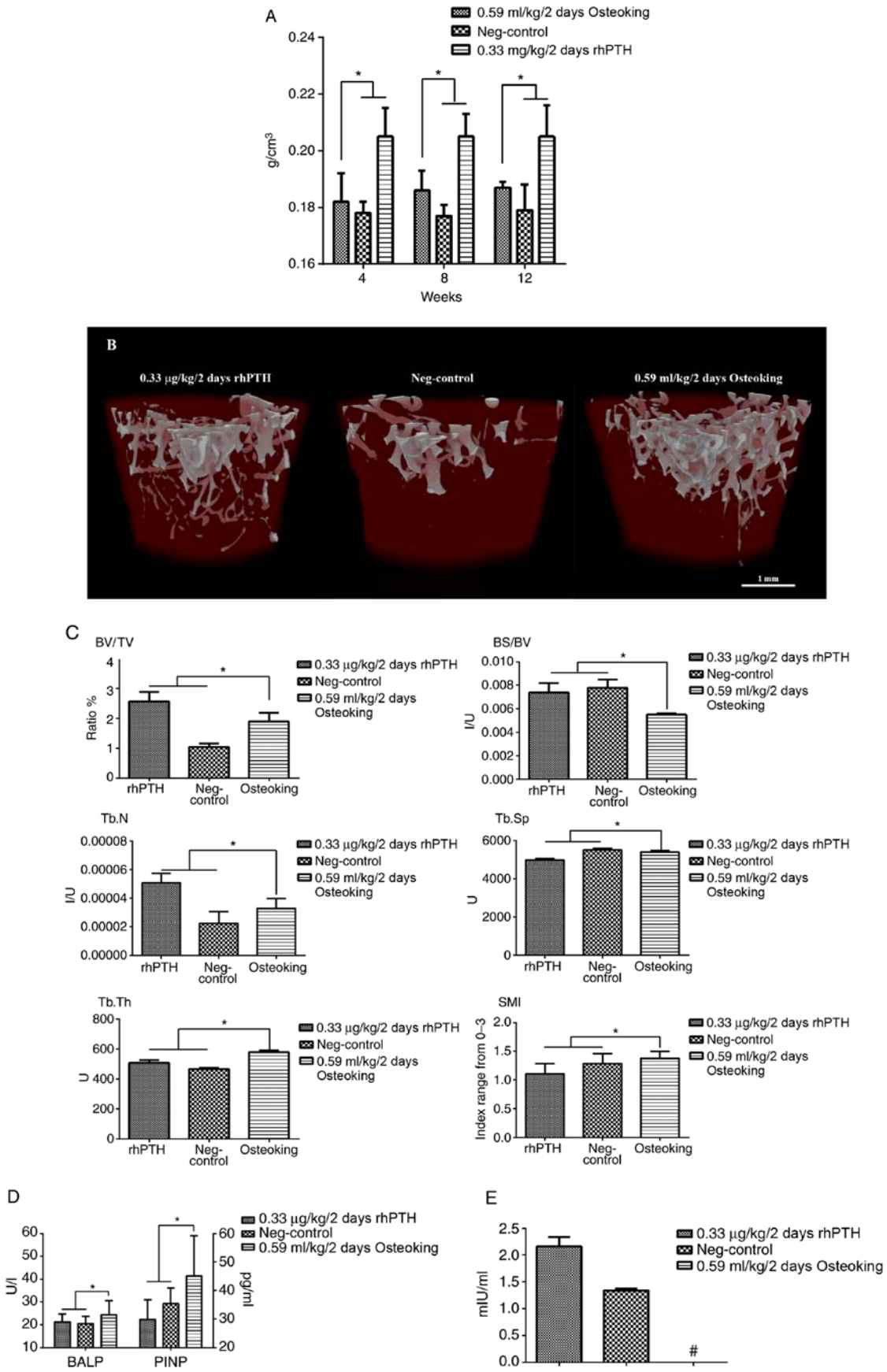

Figure 4. Osteoking leads to calcium deposition in osteoporotic rats. (A) Bone mineral density after 4, 8, and 12 weeks of administration. The values are expressed as the mean ± SD (n=6). *P<0.05. (B) Micro-computed tomography results of femurs. Scale bar=1 mm. (C) Bone composition parameters. The values are expressed as the mean ± SD (n=6). *P<0.05. (D) ELISA results of BALP and PINP after 12 weeks of administration. The values are expressed as the mean ± SD (n=6; *P<0.05; SD, standard deviation; BALP, bone alkaline phosphatase; PINP, procollagen I N-terminal peptide). (E) ELISA results of TRACP-5β after 12 weeks of administration. #, represents the value is out of the ELIASA sensitivity. The values are expressed as the mean ± SD (n=6 *P<0.05; TRACP-5β, tartrate-resistant acid phosphatase-5β).

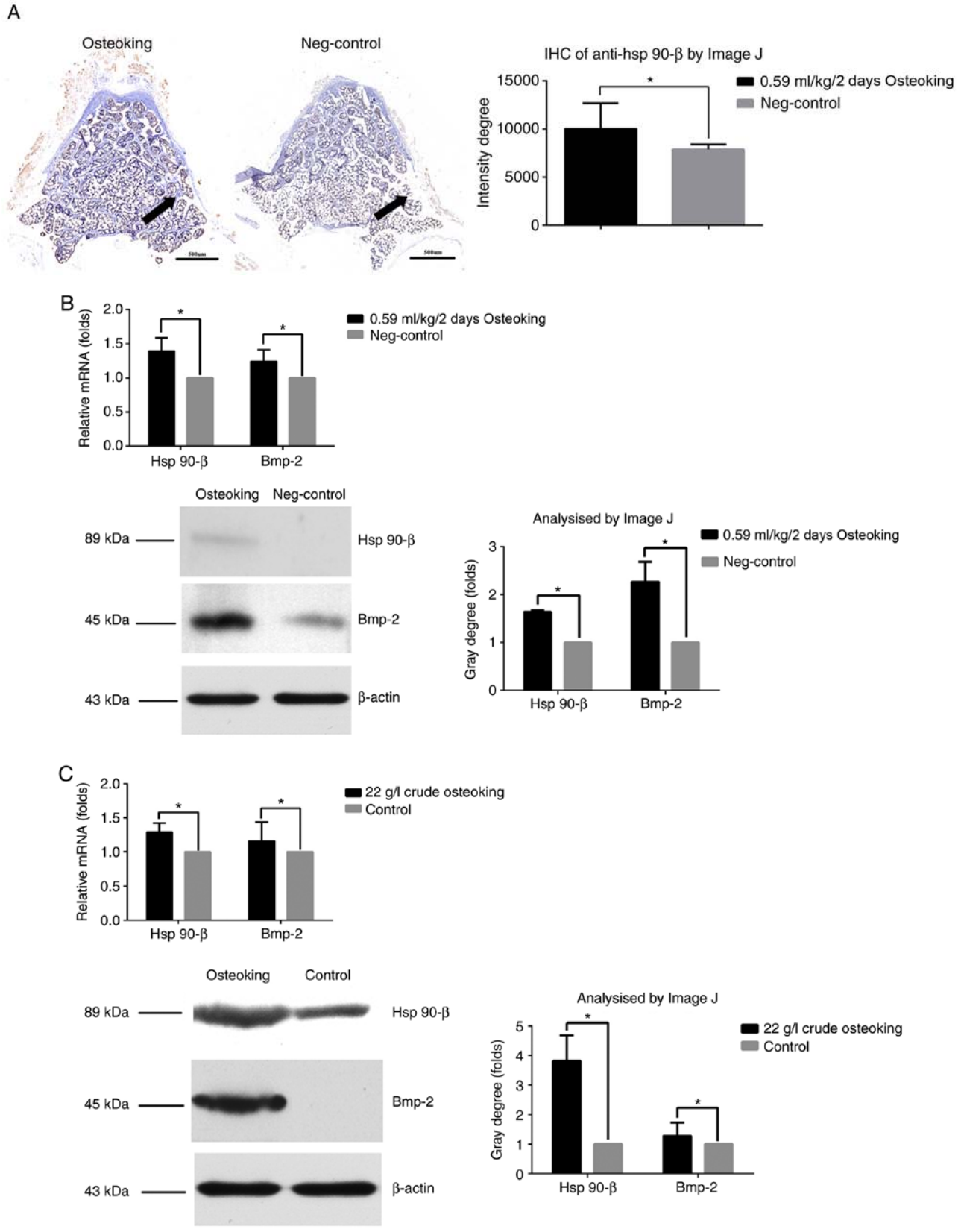

Figure 5. High HSP90-β expression enhances BMP-2 expression *in vivo* and *in vitro*. (A) IHC staining for anti-HSP90-β in the 3rd lumbar vertebra. The arrows denote the positive HSP90-β staining sections in the third lumbar vertebra. (B and C) The RT-qPCR and western blot analysis results after (B) 12 and (C) 4 weeks of administration *in vivo*. The values are expressed as the mean ± standard deviation (n=6). *P<0.05. HSP90-β, heat shock protein HSP 90-β; BMP, bone morphogenic protein; IHC, immunohistochemical; RT-qPCR, reverse transcription-quantitative polymerase chain reaction; Neg-control; negative control.

levels *in vitro*, and inhibition of HSP90-β decreased calcium deposition. These data suggest that high HSP90-β is associated with increased calcification in the osteoking group, inferring that osteoking likely improves OP by regulating HSP90-β.

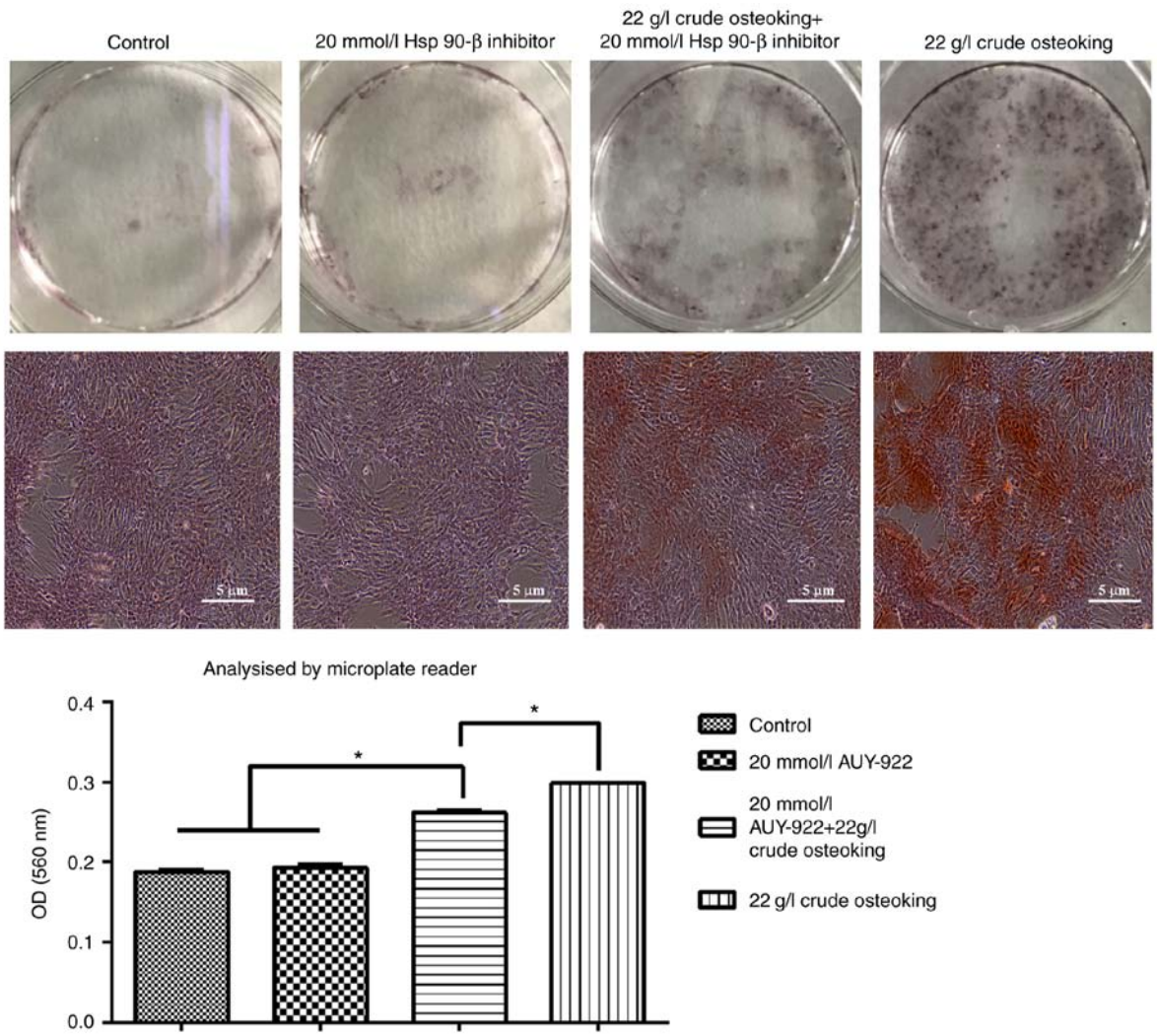

Figure 6. Inhibition of HSP90-β decreases calcium deposition. The alizarin red staining intensities in osteoblasts was measured using a microplate reader. The values are expressed as the mean ± standard deviation (n=6). *P<0.05. Scale bar=5 μM. HSP90-β, heat shock protein HSP 90-β; BMP, bone morphogenic protein; OD, optical density.

HSP90-β has been reported to contribute to the cell cycle, proliferation, migration and apoptosis (35). HSP90-β affects endothelial cells and their isoforms to promote angiogenesis (36,37). By contrast, an HSP90-β inhibitor inhibited tumor growth through apoptosis, inducing cell cycle arrest and downregulating target proteins (38,39). In addition, HSP90-β has been demonstrated to regulate bone metabolism (40).

Firstly, the present study revealed that osteoking directly stimulated rBMSCs, and that the increased HSP90-β expression was a reaction to the drug (41). These results suggest that high HSP90-β expression was not just a response to the drug, as osteoking promoted rBMSC proliferation *in vitro* (Fig. S3).

Hsp 70 promotes calcium deposition by binding to matrix Gla protein (Mgp), and Pro64 and Gla residues are required for this binding (42). HSP90-β has similar domains to those of Hsp 70, and HSP90-β binding to Mgp was investigated. Notably, the molecular interaction results did not suggest that HSP90-β binds to Mgp (Fig. S4).

Bioinformatics analysis indicated that the BMP signaling pathway was associated with the mechanism of action of osteoking. *In vivo* and *in vitro* data demonstrated that high HSP90-β was accompanied by high BMP-2 levels. High BMP-2 levels led to calcium deposition and osteogenesis. Low-intensity pulsed ultrasound, heating and cyclic tension have been reported to promote osteogenesis through upregulation of the HSP90 and BMP signaling pathways. High expressions of HSP90-β and BMP-2 was a common phenomenon of physical treatments for OP. HSP90-β promotes osteogenesis by enhancing BMP-2 (43,44).

In clinical settings, HSP90-β inhibitors have demonstrated potential effects on disease, in particular HSP90-β inhibitor-based suppression of tumor angiogenesis (45). HSP90-β inhibitors have been studied for the treatment of atherosclerosis, due to their effects on decreasing calcification (46). Following the inhibition of HSP90-β, decreased calcium deposition was observed in the osteoking + inhibitor group compared with that of the osteoking group. HSP90-β is an effective target of the osteoking-mediated effects on OP, and high HSP90-β expression promoted calcium deposition. However, calcium nodes were still observed following the inhibition of HSP90-β. These data suggest that other components of osteoking also promote calcium deposition.

In the *in vitro* experiments, a limitation of the present study was the lack of a positive drug group. It has been previously

reported that osteoking promoted the differentiation of BMSCs into osteoblasts, lipoblasts and chondroblasts (47). In the present study, high expression levels of HSP90-β promoted the differentiation of rBMSCs into osteoblasts. High BMP-2 expression levels leads to an improvement of the symptoms of OP (48). However, the mechanism between high expressions of HSP90-β and BMP-2 is unknown. A positive drug group could be helpful to explain the mechanism of action and further study is required. HSP90-β was an effective osteoking target that improved OP by enhancing BMP-2.

In addition, HSP90-β expression is also associated with blood circulation. Osteoblasts are more effective compared with osteoclasts in accelerating the exchange of oxygen-carbon dioxide, nutrient-toxic substances and serum, and increasing BMD (49-51). HSP90-β improves the bone microenvironment by activating angiogenesis, which should be investigated in future studies.

In conclusion, osteoking is a potential treatment for OP. Osteoking contains 7 components, and its mechanism is associated with the regulation of HSP90-β. Osteoking enhances HSP90-β expression levels and improves OP by upregulating BMP-2. Further examination of the association of HSP90-β and BMP-2 in OP would be valuable.

Acknowledgements

Not applicable.

Funding

The present study was supported by National Science Foundation of China-Yunnan Province Joint Fund (grant no. U1502227).

Availability of data and materials

The data used to support the findings of this study are available from the corresponding author upon request.

Authors' contributions

HBZ, WHL and ZQS designed this study. YS, DZ and RC performed all the experiments. YS and WHL drafted the manuscript. HBZ and ZQS gave suggestions and corrected the manuscript. All authors read and approved the final manuscript.

Ethics approval and consent to participate

This study is approved by Animal Experimental Ethical Committee of Kunming Medical University (approval no. KMMU 2015007).

Patient consent for publication

Not applicable.

Competing interests

The authors declare that they have no competing interests.

References

1. Dunnewind T, Dvortsin EP, Smeets HM, Konijn RM, Bos JHJ, de Boer PT, van den Bergh JP and Postma MJ: Economic consequences and potentially preventable costs related to osteoporosis in the Netherlands. Value Health 20: 762-768, 2017.
2. Ensrud KE and Crandall CJ: Osteoporosis. Ann Intern Med 168: 306-307, 2018.
3. McClung MR: Denosumab for the treatment of osteoporosis. Osteoporos Sarcopenia 3: 8-17, 2017.
4. Fukumoto S and Matsumoto T: Recent advances in the management of osteoporosis. F1000Res 6: 625, 2017.
5. Qaseem A, Forciea MA, McLean RM and Denberg TD; Clinical Guidelines Committee of the American College of Physicians: Treatment of low bone density or osteoporosis to prevent fractures in men and women: A clinical practice guideline update from the American college of physicians. Ann Intern Med 166: 818-839, 2017.
6. Hernlund E, Svedbom A, Ivergård M, Compston J, Cooper C, Stenmark J, McCloskey EV, Jönsson B and Kanis JA: Osteoporosis in the European Union: Medical management, epidemiology and economic burden. A report prepared in collaboration with the International Osteoporosis Foundation (IOF) and the European Federation of Pharmaceutical Industry Associations (EFPIA). Arch Osteoporos 8: 136, 2013.
7. Ramírez J, Nieto-González JC, Curbelo Rodríguez R, Castañeda S and Carmona L: Prevalence and risk factors for osteoporosis and fractures in axial spondyloarthritis: A systematic review and meta-analysis. Semin Arthritis Rheum 48: 44-52, 2018.
8. Tawaratsumida H, Setoguchi T, Arishima Y, Ohtsubo H, Akimoto M, Ishidou Y, Nagano S, Taketomi E, Sunahara N and Komiya S: Risk factors for bone loss in patients with rheumatoid arthritis treated with biologic disease-modifying anti-rheumatic drugs. BMC Res Notes 10: 765, 2017.
9. Minisola S, Cipriani C, Occhiuto M and Pepe J: New anabolic therapies for osteoporosis. Intern Emerg Med 12: 915-921, 2017.
10. Rossini M, Adami S, Bertoldo F, Diacinti D, Gatti D, Giannini S, Giusti A, Malavolta N, Minisola S, Osella G, *et al*: Guidelines for the diagnosis, prevention and management of osteoporosis. Reumatismo 68: 1-39, 2016.
11. Kanis JA, Cooper C, Rizzoli R and Reginster JY; Scientific Advisory Board of the European Society for Clinical and Economic Aspects of Osteoporosis (ESCEO) and the Committees of Scientific Advisors and National Societies of the International Osteoporosis Foundation (IOF): European guidance for the diagnosis and management of osteoporosis in postmenopausal women. Osteoporos Int 30: 3-44, 2019.
12. Management of osteoporosis in postmenopausal women: 2010 position statement of the North American Menopause Society. Menopause 17: 25-54; quiz 55-26, 2010.
13. Dai L, Wu H, Yu S, Zhao H, Xue L, Xu M, Shen Z and Hu M: Effects of OsteoKing on osteoporotic rabbits. Mol Med Rep 12: 1066-1074, 2015.
14. Fan L, Ma J, Chen Y and Chen X: Antioxidant and antimicrobial phenolic compounds from Setaria viridis. Chem Nat Compounds 50: 433-437, 2014.
15. Hu M, Zhao HB, Qian CY, *et al*: Ultrastructural evaluation of the SANFH rabbit animal models intervened by Osteoking. Chin J Tradit Chin Med Pharm 26: 486-489, 2011 (In Chinese).
16. Zhao HB, Hu M and Liang HS: Experimental study on osteoking in promoting gene expression of core binding factor alpha 1 in necrotic femoral head of rabbits. Zhongguo Zhong Xi Yi Jie He Za Zhi 26: 1003-1006, 2006 (In Chinese).
17. Zhao H, Hu M, Wang W and Li L: Effects of the VEGF gene expressions of Osteoking in the treatment of femoral head necrosis. China J Orthop Traumatol 20: 757-759, 2007.
18. Zhao HB, Hu M, Zheng HY, Liang HS and Zhu XS: Clinical study on effect of Osteoking in preventing postoperational deep venous thrombosis in patients with intertrochanteric fracture. Chin J Integr Med 22: 297-299, 2005.
19. Yan S: The effect of Osteoking on ovariectomized female rat model of Osteoporosis in Chinese. Chin J Osteoporosis 12: 21-24, 2016.
20. Hu M, Zhao HB, Wang B, Liang HS, Zhang CQ, Zheng HY and Zhao XL: Clinical observation on promoting effect of henggu gushang union agent on post-operational healing of Gosselin's fracture. Zhongguo Zhong Xi Yi Jie He Za Zhi 2: 160-161, 2005 (In Chinese).

21. Hasan S, Bonde BK, Buchan NS and Hall MD: Network analysis has diverse roles in drug discovery. Drug Discov Today 17: 869-874, 2012.
22. Keiser MJ, Setola V, Irwin JJ, Laggner C, Abbas AI, Hufeisen SJ, Jensen NH, Kuijer MB, Matos RC, Tran TB, *et al*: Predicting new molecular targets for known drugs. Nature 462: 175-181, 2009.
23. Qin D, Zhang H, Zhang H, Sun T, Zhao H and Lee WH: Anti-osteoporosis effects of osteoking via reducing reactive oxygen species. J Ethnopharmacol 244: 112045, 2019.
24. Jones-Bolin S: Guidelines for the care and use of laboratory animals in biomedical research. Curr Protoc Pharmacol Appendix 4: Appendix 4B, 2012.
25. Ahlquist RP: Experimental methods in pharmacology. J Pharm Sci 59: 728, 2010.
26. Morgan SL and Prater GL: Quality in dual-energy X-ray absorptiometry scans. Bone 104: 13-28, 2017.
27. Clough E and Barrett T: The gene expression omnibus database Methods Mol Biol 1418: 93-110, 2016.
28. Gage GJ, Kipke DR and Shain W: Whole animal perfusion fixation for rodents. J Vis Exp: 3564, 2012.
29. Bouxsein ML, Boyd SK, Christiansen BA, Guldberg RE, Jepsen KJ and Müller R: Guidelines for assessment of bone microstructure in rodents using micro-computed tomography. J Bone Miner Res 25: 1468-1486, 2010.
30. The UniProt Consortium: The universal protein knowledgebase. Nucleic Acids Res 45: D158-D169, 2017.
31. NCBI Resource Coordinators: Database resources of the National Center for Biotechnology Information. Nucleic Acids Res 46: D8-D13, 2018.
32. Kibbe WA: OligoCalc: An online oligonucleotide properties calculator. Nucleic Acids Res 35 (Web Server issue): W43-W46, 2007.
33. Livak KJ and Schmittgen TD: Analysis of relative gene expression data using real-time quantitative PCR and the 2(-Delta Delta C(T)) method. Methods 25: 402-408, 2001.
34. Guo XL, Liu LZ, Wang QQ, Liang JY, Lee WH, Xiang Y, Li SA and Zhang Y: Endogenous pore-forming protein complex targets acidic glycosphingolipids in lipid rafts to initiate endolysosome regulation. Commun Biol 2: 59, 2019.
35. Zuehlke AD, Moses MA and Neckers L: Heat shock protein 90: Its inhibition and function. Philos Trans R Soc Lond B Biol Sci 373: 20160527, 2018.
36. Yan X, Hui Y, Hua Y, Huang L, Wang L, Peng F, Tang C, Liu D, Song J and Wang F: EG-VEGF silencing inhibits cell proliferation and promotes cell apoptosis in pancreatic carcinoma via PI3K/AKT/mTOR signaling pathway. Biomed Pharmacother 109: 762-769, 2019.
37. Saryeddine L, Zibara K, Kassem N, Badran B and El-Zein N: EGF-induced VEGF exerts a PI3K-dependent positive feedback on ERK and AKT through VEGFR2 in hematological in vitro models. PLoS One 11: e0165876, 2016.
38. Yasui H, Hideshima T, Ikeda H, Jin J, Ocio EM, Kiziltepe T, Okawa Y, Vallet S, Podar K, Ishitsuka K, *et al*: BIRB 796 enhances cytotoxicity triggered by bortezomib, heat shock protein (Hsp) 90 inhibitor, and dexamethasone via inhibition of p38 mitogen-activated protein kinase/Hsp27 pathway in multiple myeloma cell lines and inhibits paracrine tumour growth. Br J Haematol 136: 414-423, 2007.
39. Khong T and Spencer A: Targeting HSP90 induces apoptosis and inhibits critical survival and proliferation pathways in multiple myeloma. Mol Cancer Ther 10: 1909-1917, 2011.
40. Miyasaka M, Nakata H, Hao J, Kim YK, Kasugai S and Kuroda S: Low-intensity pulsed ultrasound stimulation enhances heat-shock protein 90 and mineralized nodule formation in mouse calvaria-derived osteoblasts. Tissue Eng Part A 21: 2829-2839, 2015.
41. Tash JS, Chakrasali R, Jakkaraj SR, Hughes J, Smith SK, Hornbaker K, Heckert LL, Ozturk SB, Hadden MK, Kinzy TG, *et al*: Gamendazole, an orally active indazole carboxylic acid male contraceptive agent, targets HSP90AB1 (HSP90BETA) and EEF1A1 (eEF1A), and stimulates Il1a transcription in rat Sertoli cells. Biol Reprod 78: 1139-1152, 2008.
42. Yao Y, Watson AD, Ji S and Bostrom KI: Heat shock protein 70 enhances vascular bone morphogenetic protein-4 signaling by binding matrix Gla protein. Circ Res 105: 575-584, 2009.
43. Zhang Z, Ma Y, Guo S, He Y, Bai G and Zhang W: Low-intensity pulsed ultrasound stimulation facilitates in vitro osteogenic differentiation of human adipose-derived stem cells via up-regulation of heat shock protein (HSP)70, HSP90, and bone morphogenetic protein (BMP) signaling pathway. Biosci Rep 38: BSR20180087, 2018.
44. Chung E, Sampson AC and Rylander MN: Influence of heating and cyclic tension on the induction of heat shock proteins and bone-related proteins by MC3T3-E1 cells. Biomed Res Int 2014: 354260, 2014.
45. Graner MW: HSP90 and immune modulation in cancer. Adv Cancer Res 129: 191-224, 2016.
46. Vázquez-Carrera M: HSP90 inhibitors as a future therapeutic strategy in diabetes-driven atherosclerosis. Clin Investig Arterioscler 29: 67-68, 2017 (In English, Spanish).
47. Yu C, Dai L, Ma Z, Zhao H, Yuan Y, Zhang Y, Bao P, Su Y, Ma D, Liu C, *et al*: Effect of Osteoking on the osteogenic and adipogenic differentiation potential of rat bone marrow mesenchymal stem cells in vitro. BMC Complement Altern Med 19: 36, 2019.
48. Huang K, Wu G, Zou J and Peng S: Combination therapy with BMP-2 and psoralen enhances fracture healing in ovariectomized mice. Exp Ther Med 16: 1655-1662, 2018.
49. Griffith JF, Wang YX, Zhou H, Kwong WH, Wong WT, Sun YL, Huang Y, Yeung DK, Qin L and Ahuja AT: Reduced bone perfusion in osteoporosis: Likely causes in an ovariectomy rat model. Radiology 254: 739-746, 2010.
50. Ding WG, Wei ZX and Liu JB: Reduced local blood supply to the tibial metaphysis is associated with ovariectomy-induced osteoporosis in mice. Connect Tissue Res 52: 25-29, 2011.
51. Peng J, Lai ZG, Fang ZL, Xing S, Hui K, Hao C, Jin Q, Qi Z, Shen WJ, Dong QN, *et al*: Dimethyloxalylglycine prevents bone loss in ovariectomized C57BL/6J mice through enhanced angiogenesis and osteogenesis. PLoS One 9: e112744, 2014.

This work is licensed under a Creative Commons Attribution-NonCommercial-NoDerivatives 4.0 International (CC BY-NC-ND 4.0) License.